# 2

# *An HI Absorption study of optically selected Interstellar Clouds*

In the fi eld of observation,
chance favors the prepared mind.

—Louis Pasteur

## *Summary and the main results of chapter 2*

*Nearby interstellar clouds with high random velocities ($|v| \gtrsim$ 10 km $s^{-1}$), although easily detected in NaI and CaII lines have hitherto not been detected (in emission or absorption) in the HI 21cm line. In this chapter, we describe deep Giant Meterwave Radio Telescope (GMRT) HI absorption observations toward radio sources located at small angular separation from bright O and B stars whose spectra reveal the presence of intervening high random velocity CaII absorbing clouds.*

*The main results obtained from this study are:*

- ***In 5 out of the 14 directions searched, we detect HI 21cm absorption features from these clouds.***
- ***These are the first detections of HI absorption from the high random velocity clouds***
- ***The mean optical depth of these detections is $\sim$ 0.09, consistent with absorption arising from the cold neutral medium in the Interstellar medium.***

## 2.1 INTRODUCTION

The detection of Interstellar gas was made by Hartmann in 1904, from the observations of H & K ($\lambda \sim 3958$ Å) absorption lines of singly ionized Calcium (CaII) towards bright, high temperature stars. Narrow lines, indicating cooler origins, as compared to the hot surroundings of the stars and the observed Doppler velocities which are different from the relative velocity of the star indicated their interstellar origin. In addition, the lines seen towards binary stars showed no indication of periodic shift in frequency seen in stellar lines, which are indicative of the orbital motion of the stars. This was an added evidence for the interstellar nature of the absorbing gas. Later, in 1919, Interstellar D lines ($\lambda \sim 6000$ Å) of neutral sodium (NaI) was observed in absorption towards stars. It turns out that these are the only two species of atoms that can produce strong enough absorption in the visible region of the electromagnetic spectrum to enable intensive study by astronomers. In the case of hot stars, owing to the high surface temperature, Calcium and Sodium exists in a highly ionized state near the star. Therefore, the detected absorption lines of NaI and CaII are almost entirely interstellar.

The notion of the Interstellar medium (ISM) evolved gradually. In an important theoretical investigation, Eddington (1926) proposed a truly interstellar origin for these lines, as opposed to their origin in stellar atmospheres. Further observations and surveys in the next decade agreed with Eddington's results. The radial velocities of CaII absorption lines towards all the hot stars indicated a Galactic rotation shift corresponding to half the distance to the star, which implied a uniform distribution of the Interstellar gas. However, the fact that the widths of the lines were not correlated with the Galactic co-ordinates of the line of sight suggested that differential Galactic rotation is not the cause for line widths. This evidence suggested a "discrete cloud" model for the Interstellar medium, which has remained unchanged till now. The cloud model received support from studies of Interstellar reddening caused by intervening dust towards the stars. Extensive studies were undertaken later. The most famous of such investigations is that by Adams (1949), who used the CaII absorption spectra towards 300 stars to determine their radial velocities. In an equally seminal paper Blaauw (1952) used Adams' data to obtain a histogram of the random velocities of interstellar clouds, often (roughly) allowing for the contribution to their radial velocity due to the differential rotation of the Galaxy. One of Blaauw's main conclusions was that interstellar clouds have significant peculiar velocities, with the tail of the distribution extending up to 80 - 100 km s$^{-1}$. In an independent investigation, Routly & Spitzer (1952) found an interesting systematic behavior of the ratio of the column density of neutral Sodium to singly ionized Calcium ($N_{NaI}/N_{CaII}$). They found this ratio to decrease with increasing random velocity of the cloud. The ratio was less than 1 for the faster clouds ($|v| \gtrsim 20$ km s$^{-1}$), but significantly greater than 1 in clouds with smaller random velocities. This seems to suggest two "classes" of interstellar clouds: those with negligible random velocities and those with substantial random velocities ($|v| \gtrsim$ 15-20 km s$^{-1}$). This aspect is of great relevance for the studies that

form this thesis and will be discussed in detail later on.

The present models of the ISM are based on the extensive surveys of the HI 21cm-line from atomic hydrogen. The Dutch astronomer Van der Hulst predicted the detectability of this line and the discovery was announced together by Ewen & Purcell, Muller & Oort and Christiansen & Hindman in 1952. Our understanding of the ISM has been based to a large extent on the information gathered from the radio spectral line studies of HI. The ISM is optically thin (in most directions) in the HI line. Therefore, measured flux in the HI line emission directly gives the number of emitting atoms along the line of sight. In other words, the column density of the gas in the ISM can be derived from the studies of HI in emission. Towards radio continuum sources the HI line is observed in absorption. The HI emission and absorption data can be used to estimate the excitation temperature (called the spin temperature) of the absorbing gas.

A global picture of the ISM emerged from the HI emission and absorption studies (Clark, 1965; Radhakrishnan et al. 1972). According to the now widely accepted standard model, the ISM consists of relatively cool diffuse HI clouds at a spin temperature $T_s \sim 80$ K (cold neutral medium or the CNM) in pressure equilibrium with a warm, $T_s \sim 8000$ K, Intercloud medium (the warm neutral medium, WNM). The basic difference between these two phases are obvious from the HI emission and absorption spectra (Fig. 2.1) from Radhakrishnan et al. (1972). The narrow emission components (narrow line widths indicating lower temperature) are seen in absorption and arise in the CNM. The broad emission components do not have absorption counterparts, since the optical depth $\tau$ is inversely proportional to $T_s$.

Soon after the 21cm line of the hydrogen atom was discovered, there were attempts to detect atomic hydrogen in the interstellar clouds along the lines of sight studied by Adams (Habing 1968,1969; Goldstein & MacDonald 1969). Interestingly, whereas many lines of sight towards the O and B stars studied by Adams showed the presence of several clouds – some with very small random velocities, while others with larger random velocities – only the low velocity ones ($|v| \lesssim 10$ km s$^{-1}$) were seen in emission in the 21cm line. The emission occurred at velocities that agreed well with the velocities of the CaII absorption line features. For some reason, there was no emission that could be attributed to the higher (random) velocity clouds. Although this was very intriguing, after some speculations it was soon forgotten.

## 2.2 MOTIVATION AND OBJECTIVE

The study presented in this chapter forms a part of our continuing effort to detect interstellar clouds in the lines of sight to bright O and B stars in absorption in the 21cm line of neutral hydrogen. The main theme of the study described in this chapter pertains to the correspondence between the two families of interstellar clouds described in the previous section: the clouds seen in absorption in the optical lines (CaII and

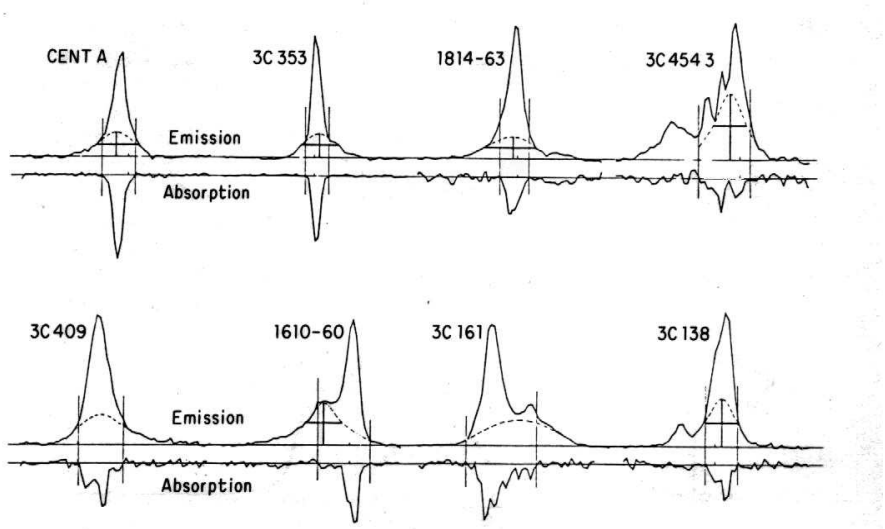


***Fig. 2.1*** Comparison of eight emission and absorption spectra from Radhakrishnan et al., (1972). The velocity limits of absorption features are marked by vertical lines. A fi t to the wide HI emission features are shown by dotted lines. These features are not found in absorption, indicating the warm nature of the gas - The Intercloud medium.

NaI) and the HI 21cm-line seen in both absorption and emission. Although the two pictures of the ISM have coexisted for decades, the question remains as to how the different subsets of clouds seen in optical are to be related to their HI counterparts. Recently Rajagopal et al. (1998a, 1998b) revived this question. Unlike in earlier 21cm studies mentioned in the previous section, they attempted to detect the atomic hydrogen in these clouds in a 21cm $absorption$ study. *They selected some two dozen stars from Adams' sample and used the VLA to do a 21cm absorption measurement against known radio sources whose angular separation from the star in question was within a few arc minutes. The idea was that such a line of sight to the radio source would pass through the same interstellar clouds that were detected earlier through the absorption lines of CaII*. Surprisingly the conclusions of this absorption study were the same as that of the earlier emission studies: **Only the clouds with random velocities less than $\sim$ 10 km s$^{-1}$ were detected in absorption and in each case the 21cm absorption velocity agreed with the velocity of the 21cm emission feature and also with the velocity of the CaII absorption line. No 21cm absorption was detected from the clouds with random velocities in excess of 10 km s$^{-1}$ down to an optical depth of 0.1.**

To explain this, Rajagopal et al. (1998b) invoked the hypothesis that the peculiar velocities of interstellar clouds was due to their encounters with expanding supernova remnants. *They argued that if this was the operative mechanism then the clouds accelerated to higher velocities would be warmer (due to their being dragged along by*

*the hot gas behind the SNR shock front) and will also have smaller column densities compared to the slower clouds (due to evaporation). This would explain the small optical depth for the 21cm absorption (which is directly proportional to the column density and inversely proportional to the temperature)*. The Routly-Spitzer effect referred to earlier, will also have a natural explanation in this hypothesis. In clouds shocked by supernova blast waves, less of Calcium is likely to be locked up in grains due to sputtering of the grains. Although shock acceleration of clouds seemed to provide satisfactory explanation, to strengthen that hypothesis it was important to observationally $establish$ a correlation between the 21cm optical depth and the peculiar velocity. The present study is a part of a continuing effort towards this end. **In this chapter, we report the results obtained from the first set of observations with the recently constructed Giant Meterwave Radio Telescope (GMRT). In these observations we obtained a limit on the optical depth roughly ten times better than that achieved by Rajagopal et al. (1998a).**

## 2.3 SOURCE SELECTION

The basic finding list of stars with the CaII absorption line data were from Adams (1949) and Welty et al. (1996). The selection criteria was that the spectra of the stars should contain both low ($|v| \lesssim$ 10 km s$^{-1}$) and high random velocity ($|v| \gtrsim$ 10 km s$^{-1}$) optical absorption features. Even though it is not possible to derive a sharp distinction between the low and the high random velocities, we have adopted the value 10 km s$^{-1}$ as the dividing line (Spitzer 1978). The distances to the stars were obtained from the HIPPARCOS catalog (1997). The background radio sources towards which we measured HI absorption were selected from the National Radio Astronomy Observatory Very Large Array Sky Survey (NVSS, Condon et al. 1996). Rajagopal et al. (1998a) chose their directions such that at half the distance to the star, the linear separation between the lines of sight towards the star and the radio source was $\sim 3$ pc. In the present observations, we have chosen the directions where this value is $< 1$ pc in most cases. This gives a better chance for both lines of sight to sample the same gas. Since our aim was to reach an rms of 0.01 in optical depth, only those radio sources with flux densities at 20cm greater than $\sim$ 100 mJy were considered, so that we could reach the target sensitivity in a reasonable integration time. However, for a few directions we compromised the separation between the lines of sight for the higher flux density of the background source. Our final list consisted of 14 fields. Table 2.1 lists a summary of the fields observed. In a few cases, there was more than one radio source within the GMRT primary beam. Four out of the fourteen stars in our list have been previously studied by Rajagopal et al. (1998) using the VLA.

***Table 2.1*** A summary of the observed directions: Column 1 lists the stars, whose spectra are known to contain high random velocity optical absorption lines. Those fields which were observed earlier by Rajagopal et al. (1998a) is marked with an asterix (*). Column 2 shows the distance to these stars obtained from the HIPPARCOS catalog. The flux density of the radio sources listed in column 6 are from the present observations. The angle $\theta$ (column 7) is the angle between the lines of sight to the star and the radio source. The linear separation between the two lines of sight at half the distance to the star is given in column 8.

| Star | d pc | l deg | b deg | Radio source | S mJy | $\theta$ | r pc |
|---|---|---|---|---|---|---|---|
| HD 175754* | 680.0 | 16.46 | −10.02 | NVSS J1856−192 | 67 | $28'$ | 2.8 |
| HD 159561 | 14.3 | 35.90 | +22.58 | NVSS J1732+125 | 174 | $41'$ | 0.1 |
| HD 166182 | 467.3 | 47.42 | +18.03 | NVSS J1809+208 | 383 | $13'$ | 0.9 |
| HD 193322 | 476.2 | 78.10 | +2.78 | NVSS J2019+403 | 310 | $28'$ | 1.9 |
| HD 199478* | 2857 | 87.51 | +1.42 | NVSS J2056+475 | 180 | $8'$ | 3.3 |
| HD 21278* | 174.8 | 147.52 | −6.19 | NVSS J0330+489 | 343 | $28'$ | 0.7 |
| | | | | NVSS J0331+489 | 189 | $22'$ | 0.6 |
| HD 24760 | 165.0 | 157.35 | −10.10 | NVSS J0400+400 | 191 | $30'$ | 0.7 |
| HD 47839 | 313.5 | 203.00 | +2.30 | NVSS J0642+098 | 340 | $8'$ | 0.4 |
| HD 37128 | 411.5 | 205.26 | −17.14 | NVSS J0536−014 | 171 | $18'$ | 1.0 |
| HD 37742* | 250.6 | 206.50 | −16.49 | NVSS J0542−019 | 408 | $7'$ | 0.3 |
| HD 37043 | 406.5 | 209.50 | −19.60 | NVSS J0535−057 | 299 | $14'$ | 0.9 |
| | | | | NVSS J0536−054 | 215 | $21'$ | 1.2 |
| HD 38771 | 221.2 | 214.52 | −18.50 | NVSS J0549−092 | 170 | $32'$ | 1.0 |
| | | | | NVSS J0549−092 | 97 | $32'$ | 1.0 |
| HD 143018 | 140.8 | 347.20 | +20.14 | NVSS J1559−262 | 328 | $10'$ | 0.2 |
| HD 147165 | 225.2 | 351.38 | +16.90 | NVSS J1623−261 | 287 | $33'$ | 1.3 |

## 2.4 OBSERVATIONS

### 2.4.1 The Giant Meterwave Radio Telescope

The Giant Meterwave Radio Telescope (GMRT) consists of 30 fully steerable dishes, of diameter 45 m with a maximum baseline of 25 km (Swarup et al. 1991). The GMRT operates as an "Earth rotation aperture synthesis telescope". The configuration of the array has been chosen in such a way as to be sensitive to both compact and extended structures of celestial radio sources. 14 antennas are placed somewhat randomly within the central one square kilometer of the array. The maximum baseline of this compact central array, known as the "central square", is $\sim$1.1 km. The shortest baseline is $\sim$100 meters. The rest of the antennas are distributed along three 14 km long arms of a "Y" shaped configuration (Fig. 2.3). This hybrid configuration provides reasonably good sensitivity for both compact as well as broad and extended sources. Apart from the Interferometric observations, the telescope can also be used as a phased array, used in the studies of pulsars.

The aperture efficiency of the dishes is $\sim 40\%$ in the 21cm band, which implies an effective area of $\sim$ 19000 m$^2$. This telescope is equipped with an FX correlator providing 128 channels per polarization per baseline. A baseband bandwidth ranging from 16 MHz down to 64 kHz variable in steps of 2 can be chosen (per sideband). The 21 cm front end receiver and the pulsar backend was built by the Raman Research Institute. The 21cm receiver is a wide band system covering the frequency range of 900 to 1450 MHz. It is a prime focus uncooled receiver with a characteristic system temperature of 70 K. The 21cm system has four sub bands, centered at 1060, 1170, 1280 and 1390 MHz, each with a 3 dB bandwidth of 120 MHz. Provision exists in the receiver to bypass the narrow bandpass filters to obtain the full 450 MHz band. Apart from the 21cm band, the telescope also operates in five other frequency bands centered at 610 MHz, 325 MHz, 233 MHz, 150 MHz and 50 MHz (under development). Fig. 2.2 shows few of the GMRT dishes.

### 2.4.2 Observing strategy

The radio observations were carried out during the period April–May, and September, 1999. Only 8–10 antennas within the central square km of the array were used. We used a baseband of width 2 MHz, which translates to $\approx$ 422 km s$^{-1}$ in velocity and a resolution of $\sim$ 3.3 km s$^{-1}$. The center of the band was set at 1420.4 MHz. The observing band was found to be free from interference. We used one of the VLA primary flux calibrators (3C48/3C147/3C286) for setting the flux density scale. We observed a nearby secondary calibrator from the VLA calibrator manual for phase and bandpass calibration. The phase calibration was carried out once every hour. Bandpass calibration was carried out once every two hours for 10 minutes with the observing frequency shifted by 2 MHz below the band, which corresponds to a velocity shift of $\approx$ 400 km s$^{-1}$. This shift is adequate to move the observing band

***Fig. 2.2*** The Giant Meterwave Radio Telescope

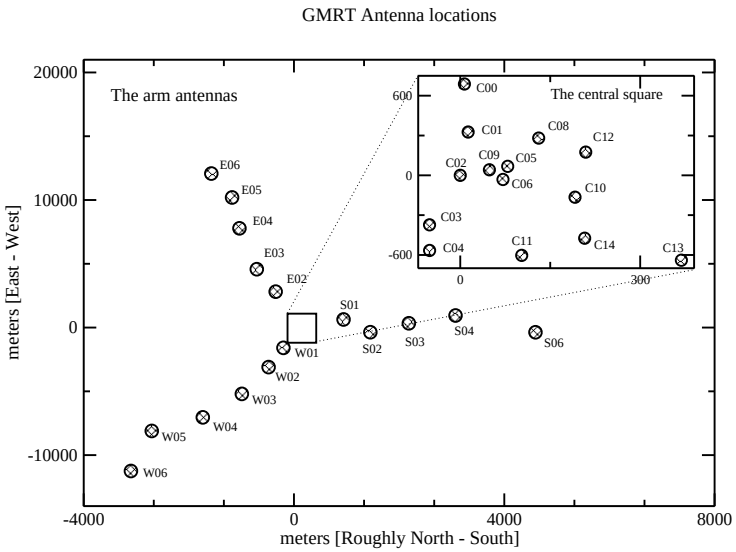


***Fig. 2.3*** The Giant Meterwave Radio Telescope: array confi guration

**Table 2.2** The Observational Setup.

| | |
|---|---|
| Telescope | GMRT |
| System temperature | $\sim 70$ K |
| Aperture efficiency | $\sim 40\%$ |
| Number of antennas | 8 to 10 |
| Base band used | 2.0 MHz |
| Number of channels | 128 |
| Velocity resolution | 3.3 km s$^{-1}$ |
| On source integration time | $\sim$ 1 to 7 hour |

out of the velocity spread of the Galactic 21cm line spectral features. On source integration time ranged from $\sim$ 1 to 7 hours, depending on the strength of the background radio source. The rms sensitivity in optical depth varied from 0.02 to 0.007 towards different sources. A summary of the observational setup is given in Table 2.2.

The analysis of the data were carried out using the Astronomical Image Processing System (AIPS) developed by the National Radio Astronomy Observatory. The resulting data set consisted of 14 image cubes containing a total of 17 HI absorption profiles. Continuum subtraction was carried out by fitting a linear baseline to the line free channels in the visibility domain and subtracting the best fit continuum from all the channels. For the point sources amongst the list of program sources, the flux densities quoted in the NVSS (Condon et al., 1996) was found to agree with the flux densities obtained from the GMRT to within 10%. Separate line images of short and long baselines were made to convince ourselves that contamination due to HI emission was minimal. The rms noise level ranged from 1.5 mJy to 5 mJy/channel/beam depending upon the integration time. **Out of the 17 directions, the lowest HI optical depth of $\sim$ 0.007 was achieved towards the source NVSS J0542$-$019**. In order to study the individual HI absorption components, multiple Gaussian profiles were fitted to the absorption line spectra using the Groningen Image Processing System (GIPSY).

## 2.5 RESULTS

We have examined the HI absorption spectra towards 14 stars having optical absorption lines at both low and high random velocities. In all these fields, we have detected HI absorption at low random velocities. In all the directions, at low random velocities ($|v| \lesssim 10$ km s$^{-1}$) there is a good agreement between the velocities of the HI absorption features and that of the CaII absorption line components, within the limits of our velocity resolution ($\sim 3.3$ km s$^{-1}$). **In 5 out of the 14 fields, for the first time, we**

**have detected HI absorption features coincident with the high random velocity CaII absorption lines**.

The 21cm absorption profiles have a typical optical depth $\tau \sim 0.1$, and a FWHM $\sim 10$ km s$^{-1}$. This velocity width is less than would be expected from thermal broadening in the WNM, and in any case, the path length of WNM required to produce an optical depth of $\sim 0.1$ is considerably larger than the distance to the star against which the NaI/CaII lines have been observed. The observed velocity width and optical depth are instead completely consistent with what would be expected from absorption in a CNM cloud. In contrast with the classical galactic emission/absorption line studies however, this cloud is too small to produce a clearly identifiable single dish emission signal. An estimate of the column density can however be obtained from the Leiden-Dwingeloo Survey (LDS) of Galactic neutral hydrogen (Hartmann & Burton 1995). The half power beam width of the Dwingeloo telescope is $\sim 36^{'}$. Hence, the column density as measured in this survey is at best indicative, since beam dilution causes it to underestimate the true $\mathrm{N}_{HI}$ of the cloud while contamination from the WNM causes it to overestimate the true $N_{HI}$. Nonetheless we have used the LDS HI column density to get a handle on the spin temperatures of the high random velocity clouds that we have detected. The $\mathrm{N}_{HI}$ was estimated by integrating over the FWHM of the HI absorption line. The same procedure was repeated for the low LSR velocity HI absorption features in the spectra and gave values that were consistent with earlier estimates. However, note that for the smaller clouds at higher velocity the fractional contribution from the WNM would be more in the HI emission spectra and would hence lead to greater errors in the estimation of $\mathrm{N}_{HI}$ and thus $\mathrm{T}_S$.

**Each of the five detections are discussed separately below**. A summary of the detections is listed in Table 2.3. Since our velocity resolution is $\sim 3$ km s$^{-1}$ and the optical absorption data for majority of the stars were obtained from a high resolution (0.3 - 1.2 km s$^{-1}$) survey (Welty et al. 1996), the number of interstellar absorption features seen in the optical study is greater than those revealed by our HI absorption study. This is evident in figures 2.3 to 2.7 which display optical depth profiles.

### 2.5.1 HI absorption detections from high random velocity clouds.

**(i) HD37043/NVSS J0535−057:** Towards the star HD37043, the high resolution CaII absorption line study by Welty et al. (1996) revealed 12 interstellar absorption features over the velocity range $-22$ to $+23$ km s$^{-1}$. The HI absorption was measured towards NVSS J0535−057, which is $14^{'}$ in projection from the star. This angular separation is equivalent to a linear separation of 0.9 pc at half the distance to the star. The HI optical depth profile shows weak but significant absorption corresponding to the high random velocity CaII absorption lines (Fig. 2.4). This weak HI absorption persists over the velocity spread of the CaII absorption lines. The HI absorption profile was fitted with 5 gaussians, centered at $+24$, $+12$, $+5$, $-2$ and $-15$km s$^{-1}$. For the direction towards this star, negative velocities are forbidden by the Galactic

***Table 2.3*** Detections of high random velocity HI absorption: Column 2 lists the high velocity ($|v| \gtrsim 10$ km s$^{-1}$) CaII absorption lines seen towards the star. Column 3 gives the radial component of the Galactic rotation velocity at the distance to the star. Column 4 gives the HI optical depth at the velocity of the CaII absorption line and Columns 5,6 and 7 list the parameters of the gaussian fit to the HI absorption profile. Column 8 lists the HI column density in the respective line of sight derived from the Leiden Dwingeloo Survey (Hartmann & Burton 1995) and Column 9 gives the derived HI spin temperature.

| Star HD no. | CaII $V_{lsr}$ (km s$^{-1}$) | $v_{Gal}$ (km s$^{-1}$) | $\tau_{HI}$ | Mean $V_{lsr}$ (km s$^{-1}$) | Peak $\tau_{HI}$ | FWHM (km s$^{-1}$) | $N_{HI}$ $\times 10^{20}$ (cm$^{-2}$) | $T_S$ (K) |
|---|---|---|---|---|---|---|---|---|
| 37043 | $-16.86$ | +2.5 | 0.12 | $-15.1$ | 0.12 | 12.8 | 0.2$^{\dagger}$ | 7$^{\dagger}$ |
| | $-12.34$ | | 0.10 | | | | | |
| | +22.68 | | 0.06 | +24.0 | 0.06 | 20.4 | 1.8 | 78 |
| 159561 | $-14.07$ | +1.9 | 0.06 | $-13.0$ | 0.06 | 11.6 | 0.5 | 40 |
| 193322 | +21.68 | +5.2 | 0.36 | +24.0 | 0.24 | 6.3 | 2.6 | 89 |
| 143018 | $-26.48$ | $-1.4$ | 0.04 | | | | | |
| | $-21.63$ | | 0.07 | | | | | |
| 24760 | +12.96 | $\sim 0$ | 0.06 | | | | | |

$^{\dagger}$: Upper limit, possibility of beam dilution.

rotation model (Brand & Blitz 1993). Presumably due to the lack of adequate velocity resolution in the 21cm spectra, the individual HI absorption features are spread over many optical absorption line components and it is difficult to obtain a one to one correspondence between them.

The HI absorption feature centered at around $-15$ km s$^{-1}$ coincides with the optical absorption line at $-16.86$ km s$^{-1}$, well within the limits of our velocity resolution. The FWHM of this HI feature is $\approx 13$ km s$^{-1}$ and the peak optical depth is $\approx 0.12$. In the LDS survey, there is no distinct HI emission feature at the velocity of the CaII and HI absorption lines, but only a shoulder of HI emission. If the gas associated with this cloud fills the Dwingeloo telescope beam, then the LDS provides an upper limit of $2.0 \times 10^{19}$ cm$^{-2}$ for the HI column density of this cloud. The upper limit on HI spin temperature implied by the $N_{HI}$ from LDS is 7 K, which is about an order of magnitude lower than typical diffuse interstellar HI clouds. It seems highly likely therefore that the high random velocity optical and HI absorption arises from a cloud much smaller in size compared to the Dwingeloo telescope beam.

**Corresponding to the CaII line at +22.68 km s$^{-1}$, the HI absorption feature at +24 km s$^{-1}$ has a derived $N_{HI} \sim 1.8 \times 10^{20}$ cm$^{-2}$ from the LDS. The implied spin temperature for this cloud is $\sim 78$ K**.

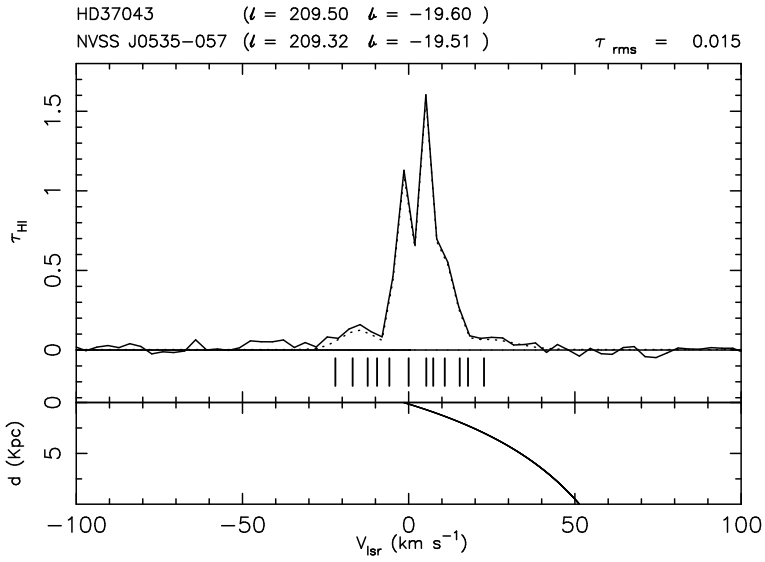


***Fig. 2.4*** The HI optical depth spectrum (solid line) towards the radio source NVSS J0535−057. The vertical tick marks indicate the velocities of the CaII absorption lines in the spectrum towards the star HD37043. The radio source and the star are separated by $14^{'}$ in the sky, which is equivalent to a linear separation of $\sim 0.9$ pc at half the distance to the star. The weak HI absorption extends over the velocity spread of the CaII absorption lines, with a distinct absorption feature at $v_{lsr} \sim -15$ km s$^{-1}$. The broken curve plotted along with the optical depth profile is the model from the Gaussian fitting to the absorption spectrum. The lower panel shows the radial component of Galactic rotational velocity for this direction as a function of heliocentric distance.

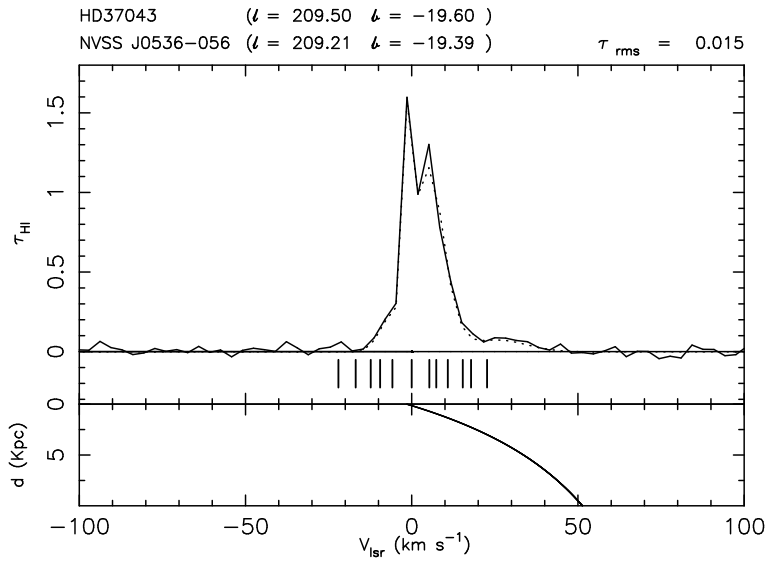


***Fig. 2.5*** The HI optical depth profi le towards the radio source NVSS J0536−054. The radio source is $\sim 21^{'}$ away in projection from the star HD37043 which implies a linear separation of $\sim 1.2$ pc at half the distance to the star. The high random velocity HI absorption feature at $\sim -15$ km s$^{-1}$ seen towards the radio source NVSS J0535−057 (Fig. 2.4) is not detected here.

*The second radio source NVSS J0536−054 in the same field of view is at an angular distance of $21^{'}$ from the star (corresponding to 1.2 pc at half the distance to the star).* Interestingly, even though HI absorption is seen over a wide range of velocities towards this source, the correlation of CaII and HI absorption line positions at higher velocities is poor (Fig. 2.5). In fact, the high velocity feature at $\sim -15$ km s$^{-1}$ seen clearly in Fig. 2.4 is absent in this figure. Obviously, this line of sight is outside the HI absorbing cloud. This lack of absorption provide a direct estimate for the size of the cloud. The upper limit to the linear size is $\sim 1.2$ pc.

**(ii) HD159561/NVSS J1732+125:** The CaII absorption line data obtained from Welty et al. (1996) indicates three interstellar CaII absorption features, one of which is at a high random velocity of $\approx -14$ km s$^{-1}$ (Fig. 2.6). The background source for the HI absorption study was NVSS J1732+125, $41^{'}$ in projection from the star. This angular extent is equivalent to a linear separation of 0.1 pc at half the distance to the star. Multiple gaussian fitting to the HI absorption profile provided 4 components, centered at $+24$, $+12$, $-0.5$ and $-13$ km s$^{-1}$. The feature at $-13$ km s$^{-1}$, with FWHM of 12 km s$^{-1}$ and a peak optical depth of $\sim$0.06 coincides with the CaII absorption line at $-14$ km s$^{-1}$. At a longitude of $36^{o}$, this velocity is forbidden by the model of Galactic rotation (Brand & Blitz 1993). Given a distance to the star $\sim 14$ pc, CaII and the HI absorption should be from a cloud in the local neighbourhood. **The HI column density estimated from the LDS is $\sim 5.3 \times 10^{19}$ cm$^{-2}$. This implies a**

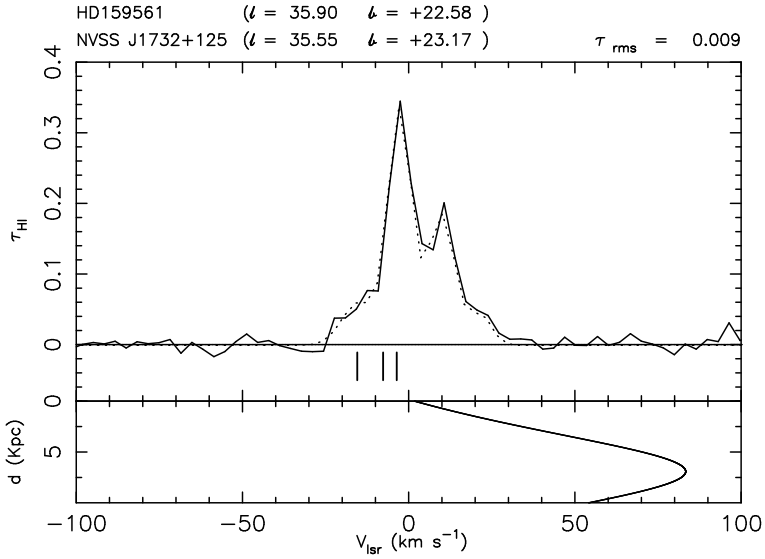


***Fig. 2.6*** The HI optical depth profile towards the radio source NVSS J1732+125. The vertical tick marks indicate the velocities of the CaII absorption lines in the spectrum towards the star HD159561. The line of sight towards the radio source is separated by $\sim 0.1$ pc from that towards the star at half the distance to the star. The HI absorption feature at $\sim -13$ km s$^{-1}$ coincides well with the CaII absorption line. The dotted curve plotted along with the optical depth profile is the model from the gaussian fitting to the absorption spectrum. The lower panel shows the radial component of Galactic rotational velocity in this direction as a function of heliocentric distance.

**spin temperature $\sim$ 40 K**.

**(iii) HD193322/NVSS J2019+403:** The star HD193322 was observed by Adams (1949) for interstellar CaII absorption lines. This direction is at a low Galactic latitude (b $\sim 2^o$) and hence the HI absorption profile towards an extra-galactic radio source can be complicated with a large number of absorption features arising from cold clouds in front of the star as well as from behind it. However it was chosen for our HI absorption study due to the presence of CaII absorption lines at velocities forbidden by the Galactic rotation. The HI absorption was measured towards NVSS J2019+403 which is $28^{'}$ in projection from the star. This angular separation is equivalent to a linear separation of about 1.9 pc at half the distance to the star. The HI optical depth profile is complicated as expected (Fig. 2.7). The absorption profile was fitted with 9 gaussian components. **There is a prominent component at an LSR velocity of $\approx$ +24 km s$^{-1}$ near the CaII absorption component at +21.68 km s$^{-1}$. The FWHM of this HI absorption feature is $\sim$ 6 km s$^{-1}$ and the peak optical depth is $\sim$ 0.24**. The $N_{HI}$ obtained from the LDS is $\sim 2.6 \times 10^{20}$ cm$^{-2}$, and the HI spin temperature $\sim$ 89 K. *However, we failed to detect HI absorption at*

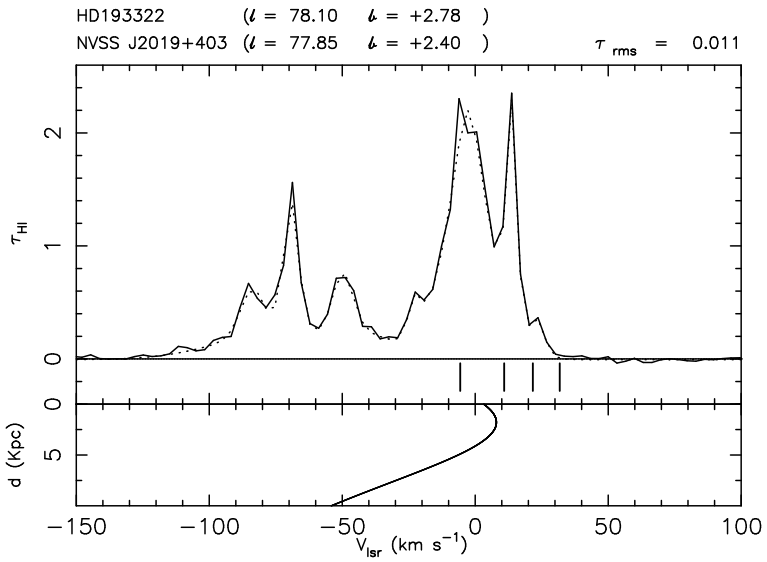


***Fig. 2.7*** The HI optical depth profile towards the radio source NVSS J2019+403. The vertical tick marks indicate the velocities of the CaII absorption lines in the spectrum towards the star HD193322, which is at an angular separation of $\sim 28^{'}$ from the radio source in the sky. The line of sight towards the radio source is separated by $\sim 1.9$ pc from that towards the star at half the distance to the star. The CaII absorption line at $\sim 23$ km s$^{-1}$ has a coincident HI absorption feature. The dotted curve plotted along with the optical depth profile is the model from the gaussian fitting to the absorption spectrum. The lower panel shows the radial component of Galactic rotational velocity in this direction as a function of heliocentric distance.

*the velocity of the CaII absorption line at +31 km s$^{-1}$ (Fig. 2.7).*

**(iv) HD143018/NVSS J1559−262:** The CaII absorption data for this star is from Welty et al. (1996). The interstellar CaII absorption lines exist at negative LSR velocities up to $-26$ km s$^{-1}$. Since the star is located at a distance of 141 pc, the radial component of Galactic rotational velocity is only $-1.4$ km s$^{-1}$ at the distance of the star. Hence, the CaII lines are arising from high random velocity clouds in the interstellar space. The HI absorption was measured towards NVSS J1559−262, $10^{'}$ in projection from the star, which implies a linear separation of 0.2 pc at half the distance to the star. An HI absorption measurement towards an extragalactic source would sample gas all along the line of sight, even beyond the star. The HI optical depth profile is shown in Fig. 2.8. It is clear from the figure that

- There is non-zero HI optical depth at the positions of the high random velocity CaII absorption lines.
- The HI absorption decreases to zero beyond the highest velocity optical absorption line component.

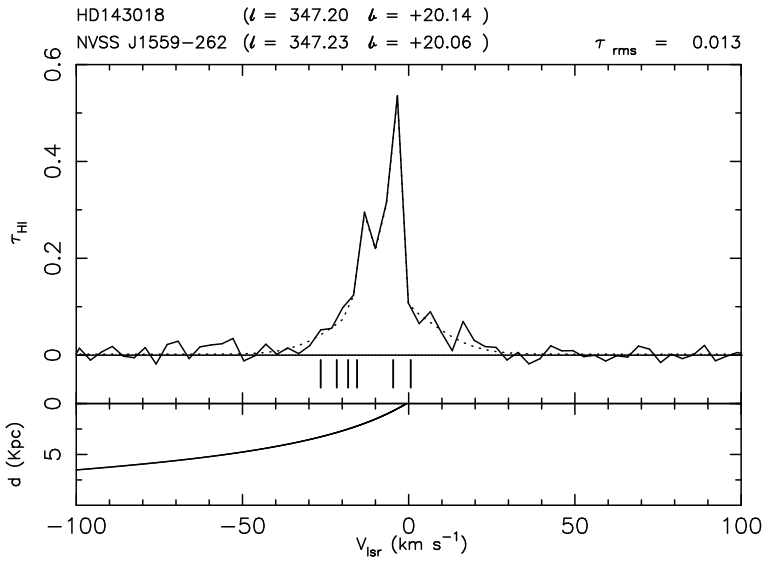


***Fig. 2.8*** The HI optical depth profile towards the source J1559−262 at a distance of $\sim 10'$ in projection from the star HD143018 The vertical tick marks indicate the velocities of the CaII absorption lines in the spectrum towards the star. The lower panel shows the radial component of Galactic rotational velocity for the direction as a function of heliocentric distance. For the latitude of this direction, any low random velocity cloud at $\sim -21$ km s$^{-1}$ should be at a distance of about 1 kpc above the Galactic plane, in the Galactic halo. Hence, any HI absorption at these velocities has to be from a nearer cloud with a large random velocity. The dotted curve plotted along with the optical depth profile is the model from the Gaussian fitting to the absorption spectra.

- For the latitude $\sim +20^o$, any low random velocity cloud (i.e. a cloud whose radial velocity is mainly due to Galactic rotation) with an LSR velocity of $\sim -21$ km s$^{-1}$ should be at a distance of about 1 kpc above the Galactic plane, which places it in the Galactic halo. This appears unlikely. It is more likely that this HI cloud is in front of the star and has a high random velocity.

The Gaussian profile fitting provided three components, at velocities $-12.5$, $-7$ and $-4.5$ km s$^{-1}$, with 5, 32 and 3.5 km s$^{-1}$ respectively as the FWHM. The existence of non zero HI optical depth at the velocities of the CaII absorption lines makes this a detection of high random velocity clouds in HI absorption but the poor signal to noise ratio prevented a faithful Gaussian fit to this data. However, the non zero HI optical depth at the positive LSR velocities, extending beyond +20 km s$^{-1}$ warrants more attention.

**(v) HD24760/NVSS J1400+400:** The CaII absorption data was obtained from Welty et al. (1996). There are 8 discrete interstellar absorption features seen in the line of CaII, out of which two at LSR velocities of $+13$ and $+16.5$ km s$^{-1}$ are at high random velocities. These velocities are forbidden by the Galactic rotation model (Brand & Blitz 1993). The HI absorption towards the radio source NVSS J1400+400, which is $30^{'}$ in projection from the star HD24760 is shown in Fig. 2.9. The HI optical depth profile indicate a non zero HI optical depth at the position of the CaII absorption line at $+13$ km s$^{-1}$, at a level of 0.06. However, as in the previous case, the gaussian fitting to this data gave no discrete component to the high velocity feature (see Table 2.3).

## 2.6 DISCUSSION

- We have obtained absorption spectra in the 21cm line of hydrogen in 14 directions which are close to the lines of sight of known bright stars against which optical absorption studies had been done earlier.
- We achieved an optical depth limit of approximately 0.01, which is about ten times better than the previous attempts in this context.
- The angular separation between the line of sight to the star and the line of sight to the radio source is also roughly two times smaller than in the earlier study.
- In 5 out of the 14 directions we have detected HI absorption at (random) velocities in excess of 10 km s$^{-1}$. To recall, in their pioneering attempt Rajagopal et al. (1998a) did not detect absorption from these faster clouds.

As mentioned earlier, our selection criteria restricted background radio sources to those with an angular separation from the star less than $\sim 40^{'}$ (implying a linear separation less than $\sim 1$ pc at half the distance to the star). In the previous 21cm absorption search (Rajagopal et al. 1998a) larger angular separations (implying linear

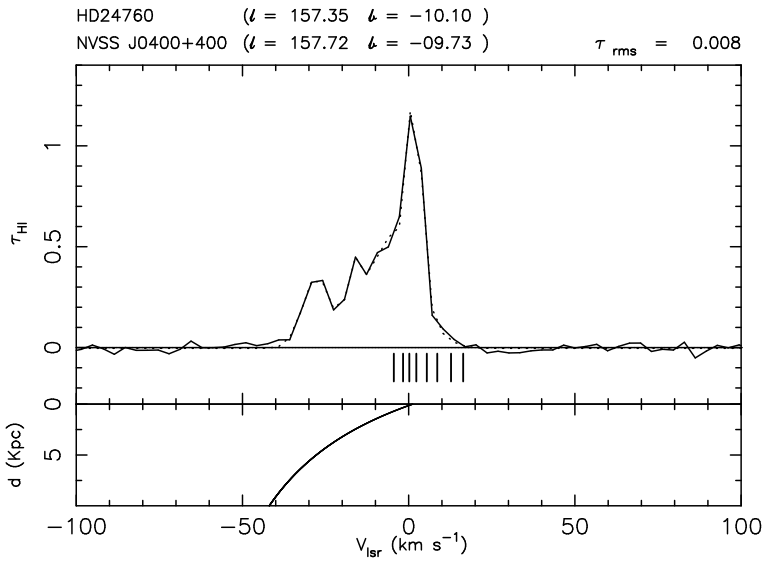


***Fig. 2.9*** The HI optical depth profile towards the source NVSS J1400+400. This radio source is separated by $\sim 30^{'}$ in projection from the star HD24760. The vertical tick marks indicate the velocities of the CaII absorption lines in the spectrum towards the star. There is a nonzero optical depth at the position of the CaII absorption line at $\sim$ +13 km s$^{-1}$. However the gaussian fitting to the HI absorption data gave no discrete component to this high velocity feature. The dotted curve plotted along with the optical depth profile shows the model from the Gaussian fitting to the absorption spectra.

separations $\sim$ 3 pc) were included in the sample. Our survey is also considerably more sensitive than that of Rajagopal et al. (1998a). Four out of the 14 directions observed in this study – the fields containing the stars HD 175754, HD 199478, HD 21278 and HD 37742 respectively – were previously studied by Rajagopal *et al.* (1998a, 1998b). The rms optical depth levels achieved in their study in these directions were 0.09, 0.21, 0.08 and 0.03, respectively. Whereas in our study, these figures are 0.03, 0.015, 0.008 and 0.007, respectively. However, we too failed to detect any HI absorption from the clouds in all these four directions. This is intriguing since the results of our study indicate that about 30% of the high random velocity clouds are detectable (5 detections out of the 14 observed directions) at the sensitivity levels reached in this study ($\tau_{HI} \sim 0.01$). We wish to point out that for two of these overlapping lines of sight (towards HD 175754 and HD 199478) the linear separation between the directions towards the radio source and that towards the star are $\sim$3 pc (Table 2.1). This value is much smaller for the rest of the directions. In addition, for one case where we do have a direct estimate for the size of the cloud (HD37043), the upper limit to the linear size is $\sim 1.2$ pc. For more than 50% of the directions studied by Rajagopal et al. (1998a, 1998b), the rms optical depth level was $above$ 0.1. The mean value of peak optical depth for our detections is $\sim$ 0.09. Only one of the fields

studied by Rajagopal et al. (1998a) had the sensitivity level to detect this optical depth.

Earlier we recalled the conclusion by Blaauw (1952) $viz.$ the distribution of random velocities of clouds extended beyond $\sim$ 80 km s$^{-1}$. But this high velocity tail seemed distinct from the rest of the distribution that was well fit by a gaussian with a dispersion of $\sim$ 5 km s$^{-1}$. Indeed, Blaauw was careful to remark on this. Later 21cm surveys of the Galaxy also yielded, as a byproduct, information about the velocities of the interstellar clouds. Unlike in the optical absorption studies towards relatively nearby stars (with good distance estimates), in the radio observation one did not have reliable distance estimates to the clouds and therefore one could not correct for the Galactic differential rotation to derive a distribution of random velocities.

## 2.7 SUMMARY AND OUTLOOK

To summarize the results obtained, we have found for the first time HI absorption from the high random velocity clouds in the ISM. Given our limited sample and the optical depth sensitivity, we cannot unambiguously state the nature of the high random velocity gas. The need to extend this to a survey towards more directions, at a deeper sensitivity level is clear. It is indeed interesting to note that until now there has been no efforts to study the distribution of observed random velocities of HI 21cm-line features and to compare it with the spectral line studies at other wavelengths. There has been no efforts to study the variation of optical depths and column densities of Interstellar HI line features with their velocities. We have carried out such a project and the next chapter will describe the observations and results from this project. In this new sample, we have used the GMRT to measure HI absorption towards 104 bright ($S_{20cm} \gtrsim$ 1Jy) radio continuum sources located away from the Galactic plane ($|b| > 15^{\circ}$).

## REFERENCES

1. Adams, W. A., 1949, Astrophys. J., 109, 354.
2. Blaauw, A., 1952, Bull. Astr. Inst. Netherland., 11, 459.
3. Brand, J., Blitz, L., 1993, Astr. Astrophys., 275, 67.
4. Clark, B.G., 1965, Astrophys. J., 142, 1398.
5. Condon, J. J., Cotton, W. D., Greisen, W. E., Yin, Q. F., Perley, R. A., Taylor, G. B., Broderick, J. J., 1996, Astron. J, 115, 1693.
6. ESA, 1997, The Hipparcos and Tycho Catalogues, ESA SP-1200.

7. Eddington, A.S. 1926, Proc. R. Soc. London, A, 111, 424.

8. Goldstein, S. J., MacDonald, D. D., 1969, Astrophys. J., 157, 1101.

9. Habing, H. J., 1968, Bull. Astr. Inst. Netherland., 20, 120.

10. Habing, H. J., 1969, Bull. Astr. Inst. Netherland., 20, 171.

11. Hartmann, D., Burton, W. B., 1995, An Atlas of Galactic Neutral Hydrogen, Cambridge Univ. Press.

12. Radhakrishnan, V., Goss, W.M., Murray, J.D., Brooks, J.W., 1972, Astrophys. J. Suppl., 24, 49.

13. Rajagopal J., Srinivasan, G., Dwarakanath, K. S., 1998a, J. Astrophys. Astr., 19, 97.

14. Rajagopal J., Srinivasan, G., Dwarakanath, K. S., 1998b, J. Astrophys. Astr., 19, 117.

15. Routly, P. M., Spitzer, L. Jr., 1952, Astrophys. J., 115, 227.

16. Spitzer, L. Jr., 1978, Physical Processes in the Interstellar Medium., New York:Wiley Interscience.

17. Swarup, G., Ananthakrishnan, S., Kapahi, V. K., Rao, A. P., Subrahmanya, C. R., Kulkarni, V. K., 1991, Current Science, 60, 95.

18. Welty, D. E., Morton D. C., Hobbs, L. M., 1996, Astrophys. J.Suppl., 106, 533.